

Problem: Protein biosynthesis takes place on free or membrane-bound ribosomes, yielding linear sequences of amino acids. In a second step, proteins acquire their singular, unique three-dimensional structure – central prerequisite for their specific functions. The rules relating the linear information stored in the DNA of an organism's genome to the amino acid sequences of the corresponding proteins are well understood. However, the complexity of the many-body interactions that govern the spontaneous transition of a polypeptide chain into its spatially ordered native conformation has to date prevented a comprehensive solution of the protein-folding problem.

Issues:

1. 1930s and 40s indicated that protein folding is autonomous and reversible, initial hope that the rules for protein folding would be simple.
2. The 1970s and 80s were dominated by the hunt for folding intermediates on the pathway from the unfolded to the native state led to the identification of structurally and spectroscopically distinct intermediate states in the folding of a large number of proteins.
3. 1990s: The discovery of small proteins that fold at very high rates (10^3 s^{-1} and faster) without populating stable intermediates. The identification of “two-state folders” very clearly demonstrated that stable intermediates are not a general prerequisite for folding.
4. New problems: Protein-folding “speed limit” and “downhill”—or barrierless—folding, the importance of unfolded-state dynamics and the prediction of protein-folding rates.
5. Uses- Realisation that the irrelevant side reactions are of great medical relevance and a probable cause of a wide range of diseases, especially neurodegenerative disorders such as Alzheimer’s, Parkinson’s, and Huntington’s disease.

But...A detailed structural understanding of the processes involved is difficult or even impossible with classical methods investigating large ensembles of molecules.

Single molecule investigations

Earlier – AFM

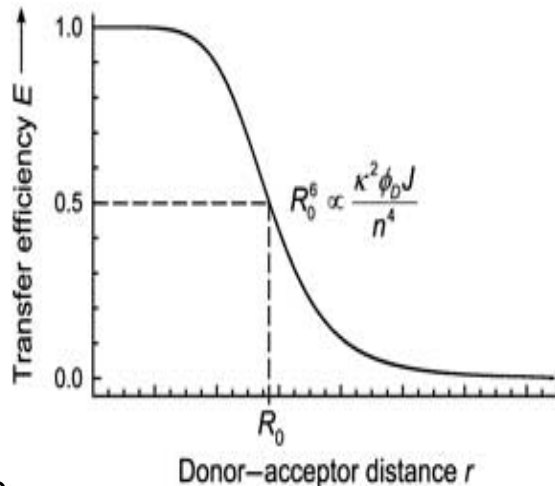
Förster Resonance Energy Transfer (FRET)

$$E = R_0^6 / [R_0^6 + r^6]$$

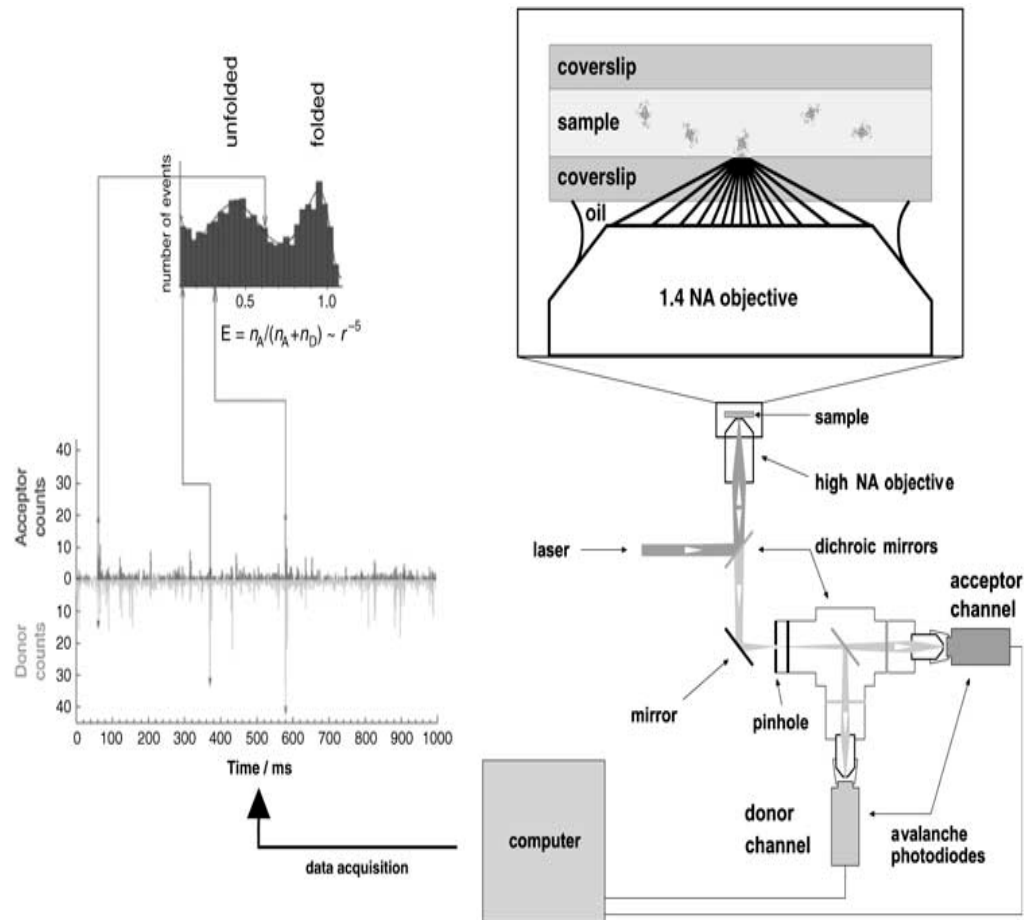
Transfer efficiency E depended on the inverse sixth power of the interchromophore distance r .

R_0 is the Förster radius, the characteristic distance that results in a transfer efficiency of 50%

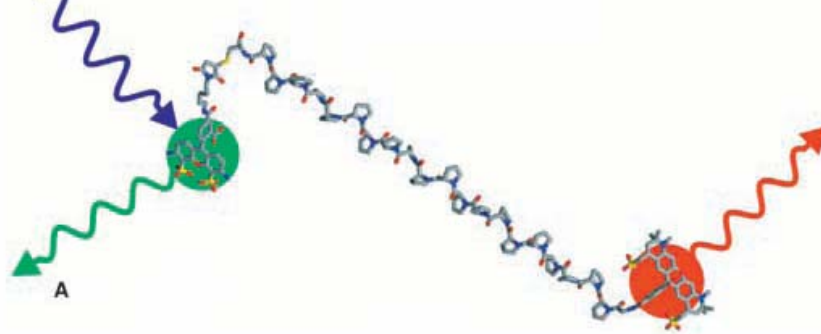
R_0 can also be calculated from theory.



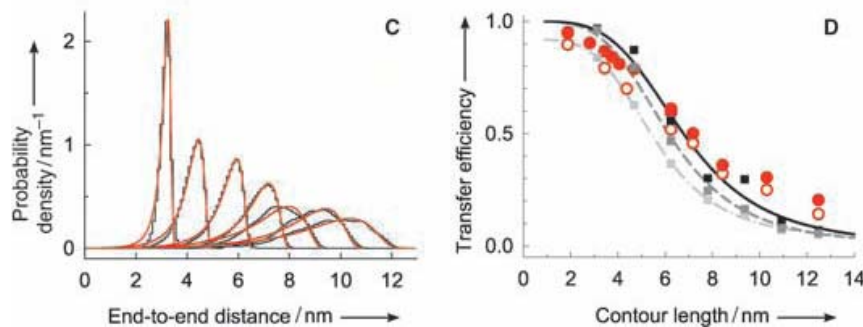
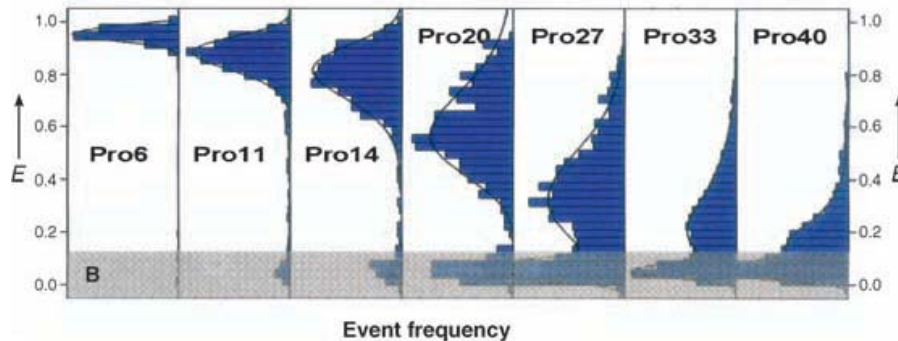
Distance dependence of the Förster resonance energy transfer efficiency between a suitable pair of chromophores. The characteristic Förster distance R_0 is calculated from the orientational factor k^2 , the donor quantum yield ϕ_D , the overlap integral J , and the refractive index of the medium n .



Scheme of a confocal single-molecule fluorescence experiment on freely diffusing molecules (molecules not to scale). On the left, a typical time trace is shown, with counts detected from the donor chromophore and the acceptor chromophore. For each individual event, a transfer efficiency is calculated and entered into a histogram. Histograms are typically constructed from several thousand bursts.

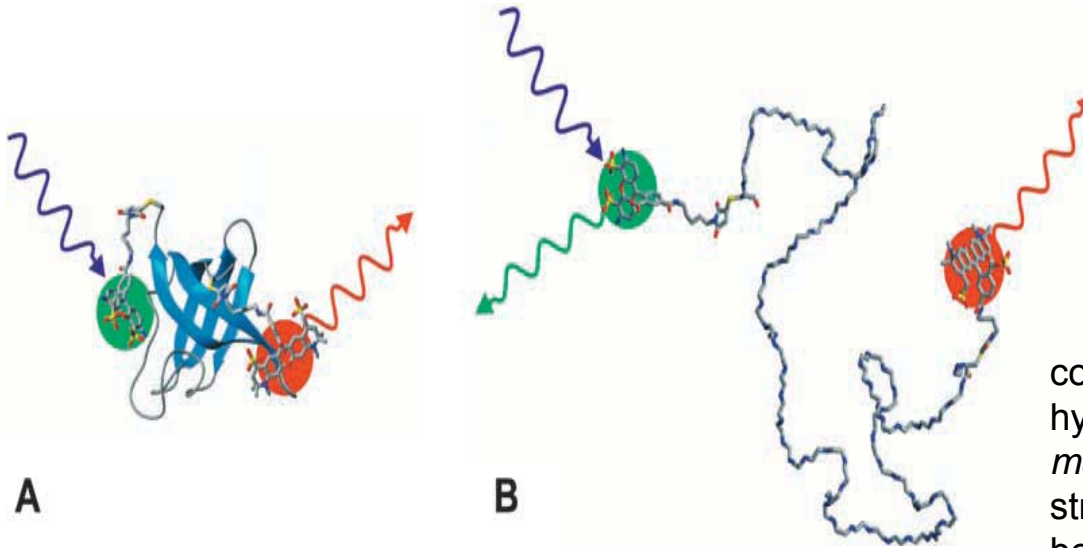


Equilibrium experiments



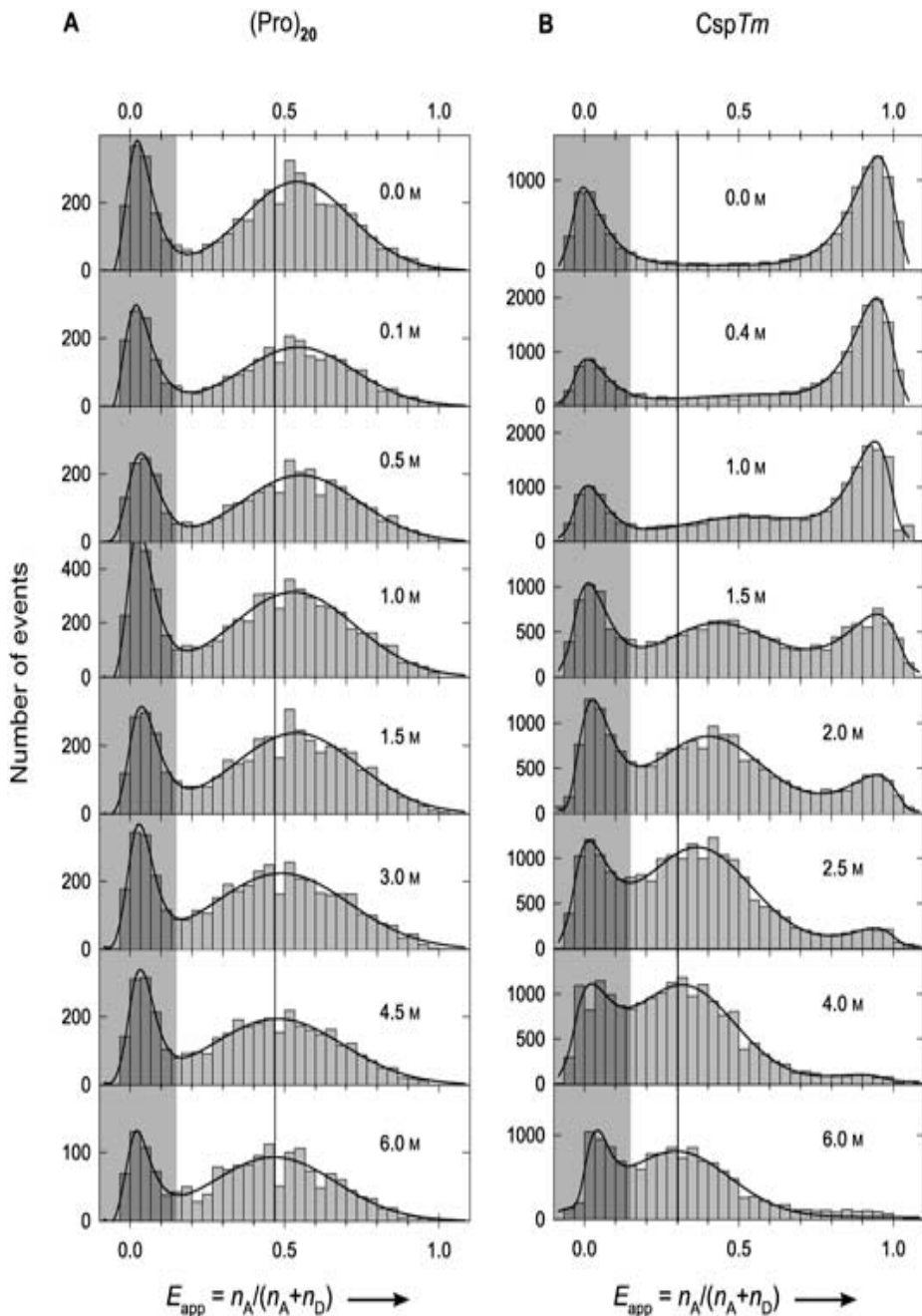
A) Schematic structure of an icosaproline helix labeled with donor (Alexa 488) and acceptor (Alexa 594) dyes. B) Transfer efficiency histograms from confocal single-molecule measurements on polyproline peptides of various lengths.[97] C) End-to-end distance distributions obtained from molecular dynamics simulations of polyproline peptides containing 10, 15, 20, 25, 30, 35, and 40 proline residues plus terminal glycine and cysteine residues (black lines) and the least-squares fits to a wormlike chain model (red lines).[97] D) Mean transfer efficiencies from single-molecule measurements (filled red circles) and ensemble time-correlated single-photon counting measurements (empty red circles) as a function of the contour lengths of the peptides (Gly–Pron–Cys), assuming the geometry of polyproline found in the crystal structure,[114] in comparison to the dependences calculated for different dynamic regimes (squares) using the normalized end-to-end distance distributions from the molecular dynamics simulations of the peptides. The black lines are empirical fits to the data.[97]

The Cold-Shock Protein



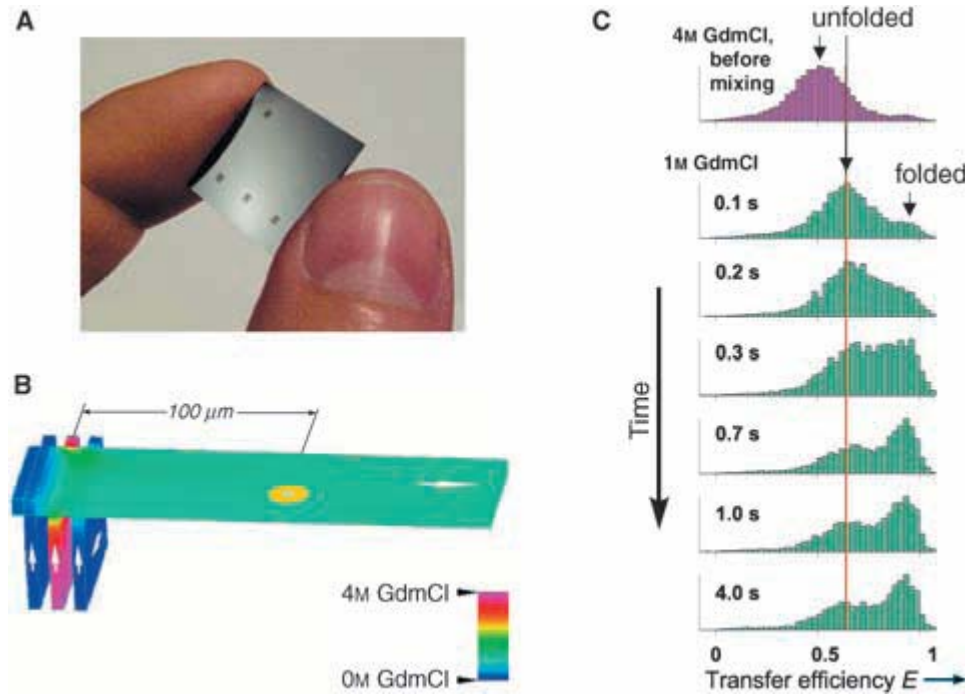
cold-shock protein from the hyperthermophilic bacterium *Thermotoga maritima* (CspTm). It forms a simple, five-stranded beta barrel structure and it behaves as a perfect two-state folding system.

Schematic structures[162] of folded and unfolded protein labeled with donor (Alexa 488) and acceptor (Alexa 594) dyes. A) Folded CspTm, a 5-stranded, 66-residue β -barrel protein (PDB-code 1G6P),[163] B) unfolded CspTm. A blue laser excites the green-emitting donor dye, which can transfer excitation energy to the red-emitting acceptor dye.



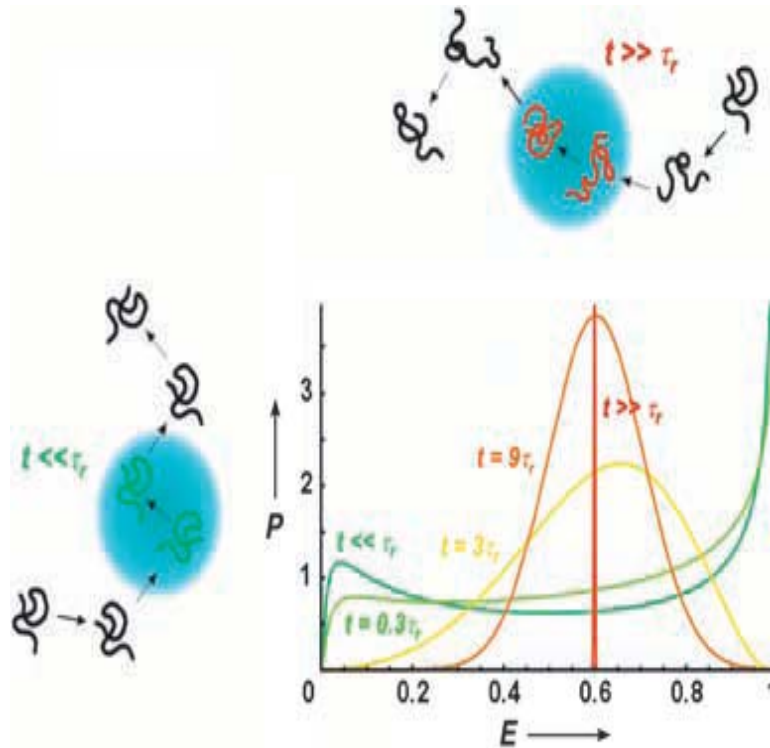
Histograms of measured FRET efficiencies at various GdmCl concentrations for labeled CspTm (A) and (Pro)20 (B). The black curves are the best fits to the data using lognormal and/or Gaussian functions. The vertical lines indicate the mean transfer efficiency of A) the unfolded subpopulation or B) (Pro)20 at 6m GdmCl. The peak at transfer efficiencies near zero (shaded in grey) is due to molecules lacking an acceptor chromophore, owing either to residual impurities or to photobleaching.

Folding Kinetics Using Microfluidic Mixing



Protein-folding kinetics studied by microfluidic mixing. A) Photograph of the mixing device. B) Schematic of the mixing area, with the three inlet channels coming in from the bottom. GdmCl concentrations calculated from its diffusion coefficient and the flow rate are indicated on a color scale. The $1/e^2$ intensity contour of the laser beam (light blue) is illustrated along with the cone of fluorescence emission collected by the microscope objective (yellow). C) Histograms of measured FRET efficiencies before (topmost panel) and at different distances downstream of the mixing area, corresponding to different times after mixing. The vertical red line indicates the mean FRET efficiency value in the unfolded state after mixing.

Chain Dynamics and the Protein-Folding “Speed Limit”



Chain dynamics and the time scale of observation. The diffusion of molecules through the focal spot is shown schematically. In one case (green), the reconfiguration time of the chain τ_r is large relative to the observation time t , resulting in a very broad transfer efficiency distribution. At the other extreme (red), τ_r is much less than t , and theoretically a delta function is expected for the transfer efficiency distribution of all molecules. Intermediate cases are shown in light green, yellow, and orange.